

# The Doppler Crisis of TeV Blazars

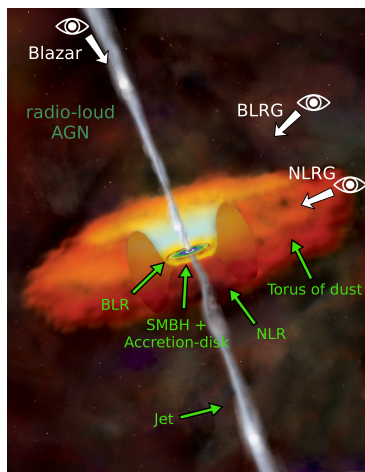
## Fermi Summer School

Amar Hekalo

June 5, 2018



# Unification Scheme



Adapted from: NASA/CXC/M.Weiss

- AGN classifications based on spectral lines, luminosity, morphology, etc.
- Unification: Only two parameters defining AGN types
  - ⇒ (radio-)luminosity
  - ⇒ inclination angle
- relativistic jet in radio-loud AGN
- Low inclination angle leads to Doppler boosting

# Radio Galaxies

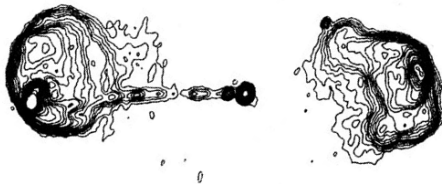
Morphological classification by Fanaroff and Riley

FR 1:  $\log(L) < 24.5$



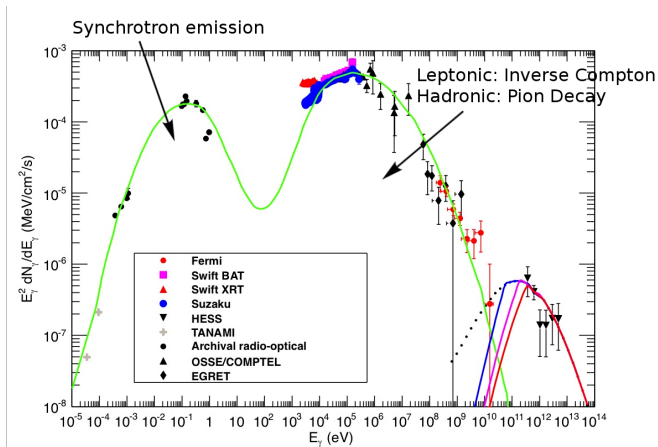
3C449 from Perley et al., 1979

FR 2:  $\log(L) > 26$



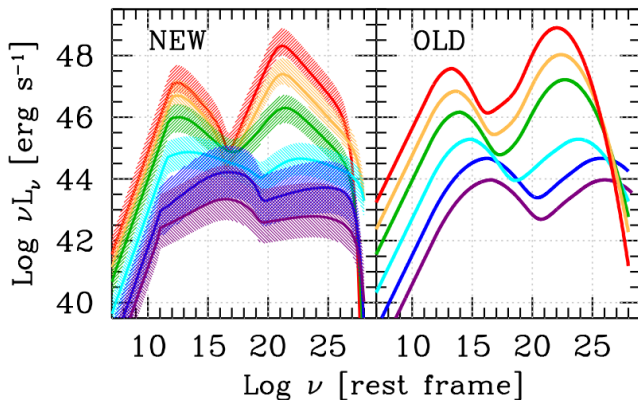
3C47 from Bridle et al., 1994

# Blazars: Spectral Energy Distribution



Adapted from: Sahu et al., 2012

# The Blazar Sequence



Credit: Ghisellini et al., 2017

- High-frequency-peaked BL Lac  $\nu_{\text{sp}} > 10^{15}$  Hz

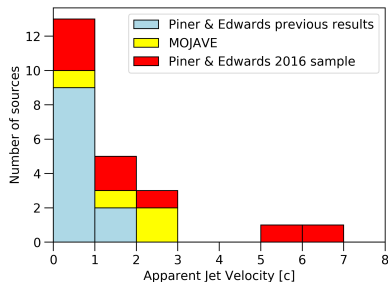


# TeV blazars: Observations

- Ground based telescopes like H.E.S.S., MAGIC and VERITAS
- Over 200 sources listed at [tevcat.uchicago.edu](http://tevcat.uchicago.edu)
- Majority of extragalactic objects are HBL
- Rapid and strong flares in several sources, e.g. PKS 2155–304, Mrk 501, Mrk 421
- Flux variability down to minutes ( $\sim 600$  s)
- Very small emitting regions  $\Rightarrow$  Heavily boosted with  $\Gamma \sim 50$  and  $\delta \sim 100$

# Kinematic studies of HBLs

- Majority of kinematic studies by Piner and Edwards
- VLBA observations at  $\sim 10\text{s GHz}$
- Slow apparent motions in all sources
- e.g. 2155-304:  
 $v_{\text{app}} = (0.93 \pm 0.31)c$
- modest brightness temperatures
- slow apparent speeds (radio) vs. high Lorentz factors ( $\gamma$ )  
 $\Rightarrow$  Doppler Crisis

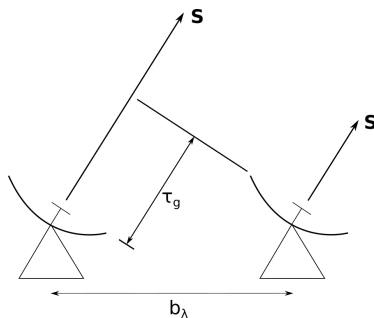


Reproduced from Piner and Edwards, 2016



# Two-Element Interferometer

Two antennas with geometrical delay  $\tau_g$  and baseline  $b_\lambda$



Interferometer measures the complex visibility:

$$V_{ij} = \int A(\sigma) B_\nu(\sigma) \exp(i2\pi b_{ij,\lambda} \times \sigma) d\Omega$$

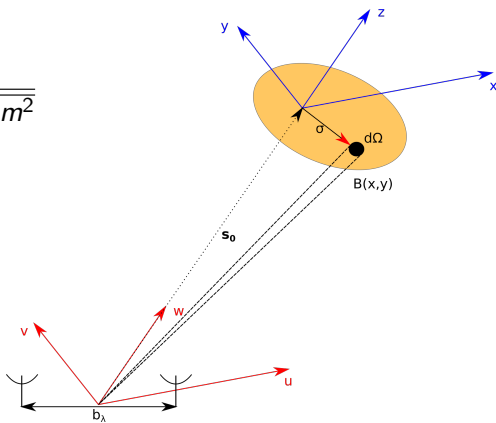
# The $(u, v)$ -plane

$$V_{ij} = \int A(l, m) B_v(l, m) \exp [i2\pi(ul + vm)] \frac{dl dm}{\sqrt{1 - l^2 - m^2}}$$

Small angle approximation:

$$V_{ij} \approx \int A(x, y) B(x, y) \exp [i2\pi(ux + vy)] dx dy$$

$$\Rightarrow B(x, y) \stackrel{\text{FT}}{\rightleftharpoons} V(u, v)$$



# Aperture Synthesis with Arrays

- Earth rotation synthesis:  
 $\delta$ -dependence
- Closure relations:
  - $\phi_{ijk} = \bar{\phi}_{ij} + \bar{\phi}_{jk} + \bar{\phi}_{ki}$
  - $A_{ijkl} = \frac{|\bar{V}_{ij}||\bar{V}_{kl}|}{|\bar{V}_{ik}||\bar{V}_{jl}|}$
- $V_{\text{measured}} =$   
 $w(u, v)W(u, v)V(u, v)$

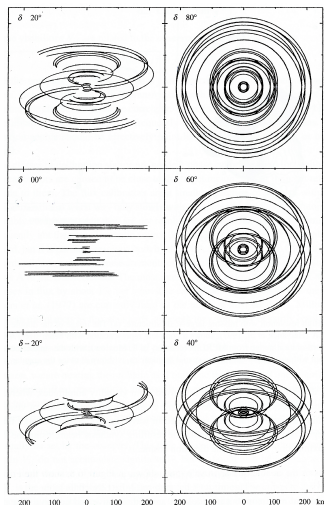
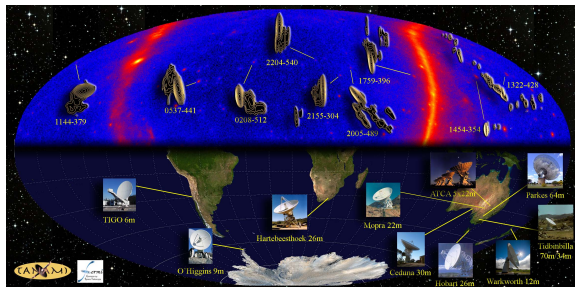


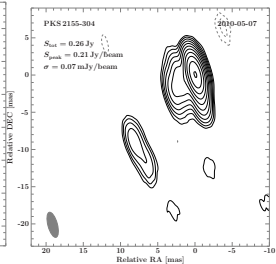
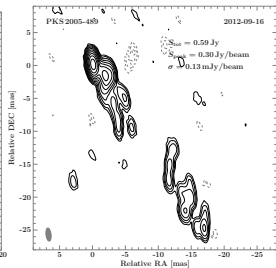
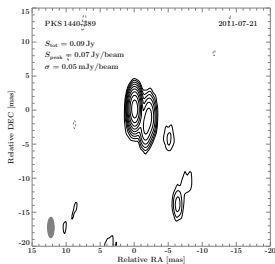
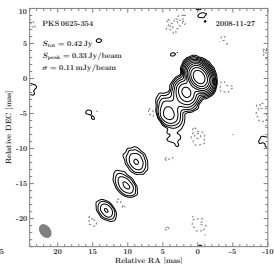
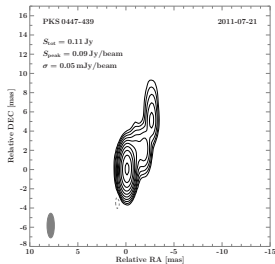
Figure: Credit: Burke and  
Graham-Smith, 2010



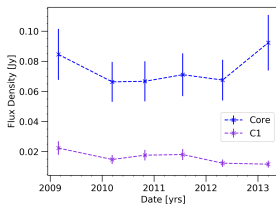
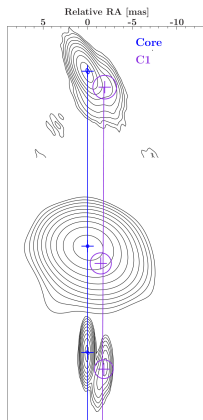
Credit: Matthias Kadler

- Tracking Active Galactic Nuclei with Austral Milliarcsecond Interferometry
- multiwavelength program with VLBI at its core
- Sample of Southern sources  $\delta < -30^\circ$

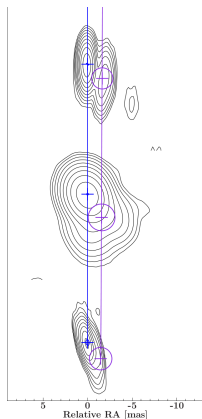
# The Sample



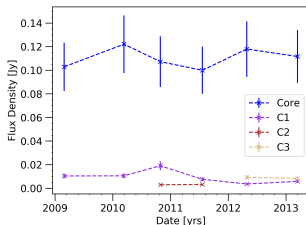
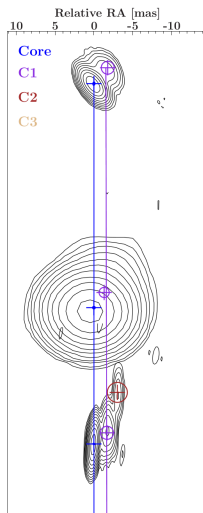
# PKS 1440–389: Kinematic analysis



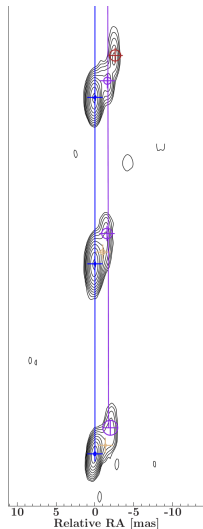
- HBL at  $0.14 < z < 2.2$
- Compact jet to southwest
- one component with  $\beta_{\text{app}} = 0.99 \pm 0.73$
- stable flux density



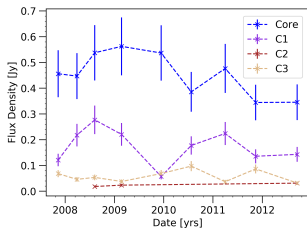
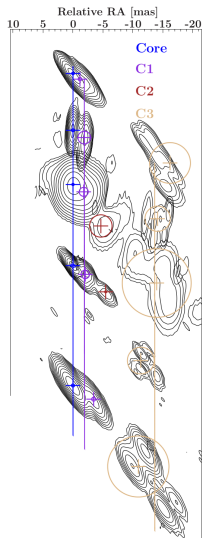
# PKS 0447–439: Kinematic analysis



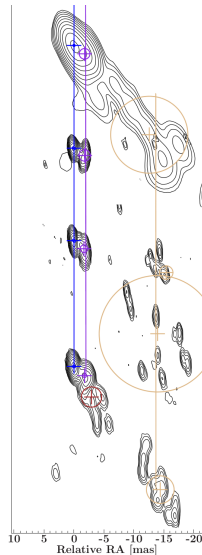
- HBL (initially Seyfert I), redshift ambiguous
- superluminal component with  $\beta_{\text{app}} = 5.4 \pm 2.5$
- stable flux density



# PKS 2005–489: Kinematic Analysis

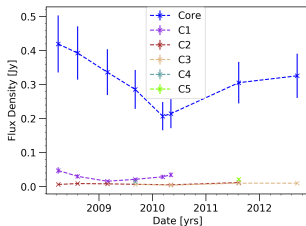
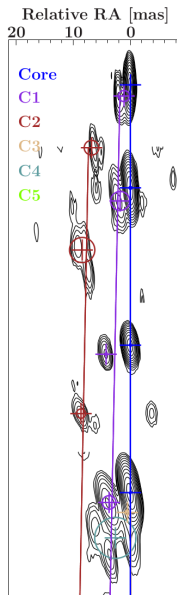


- radio flux density of  $\sim 0.56 - 0.88 \text{ Jy}$
- jet difficult to model
- inner component stationary

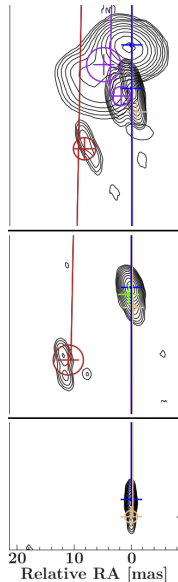




# PKS 2155–304: Kinematic Analysis

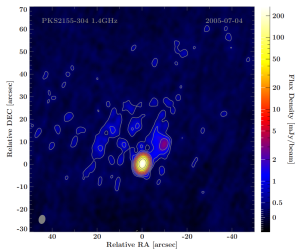


- huge flare in 2006
- variable flux density
- possible jet bending
- all comps. superluminal, fastest  $\beta_{\text{app}} = 7.8 \pm 2.5$



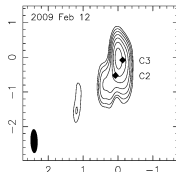
# PKS 2155–304: Jet Bending

Small-scale bending ( $\sim 75^\circ$ ) in Piner et al., 2010 and large scale bending proposed in Seeg, 2017:

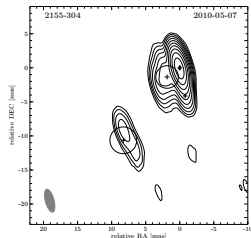


Credit: Seeg, 2017

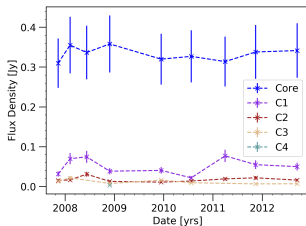
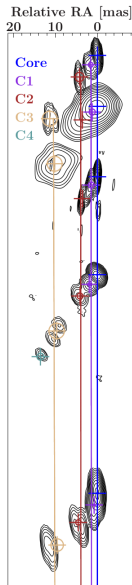
Small scale jet-bending at  
8.4 GHz  
from C3 to C1 with bending of  
 $\sim 47^\circ$



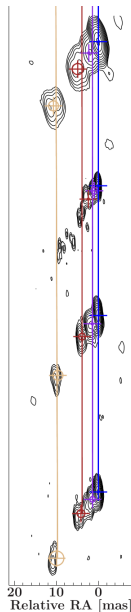
Credit: Piner et al., 2010



# PKS 0625–354: Kinematic Analysis

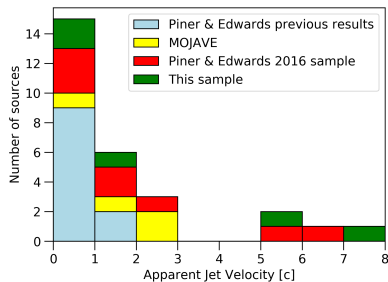


- fastest component at  $\beta_{\text{app}} = 1.07 \pm 0.89$
- morphology  $\rightarrow$  FR I, spectrum  $\rightarrow$  BL Lac
- computed inclination angle as  $\phi < 59^\circ$



# Implications for the Doppler Crisis

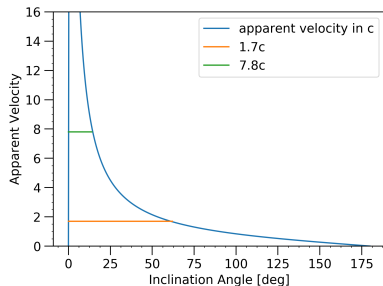
- Previous kinematic studies on HBLs done by only one group
- Goal: independent study of Southern TeV Blazars
- Result: Mostly slow and stationary, but also superluminal components
- Distribution requires more statistical analysis
- If Doppler Crisis true: How to explain the discrepancy?



Adapted from Piner and Edwards, 2016

# Problems and Models

- PKS 2155–304:  $\Gamma \sim 50$  or  $\beta_{\text{int}} \sim 0.9998$
- Plotting  $\beta_{\text{app}} = \frac{\beta_{\text{int}} \sin(\phi)}{1 - \beta_{\text{int}} \cos(\phi)}$  for two speeds of PKS 2155–304
- $\phi \ll 1^\circ \Rightarrow$  Huge linear sizes  $\sim 220$  Mpc for  $\phi \sim 0.01^\circ \Rightarrow \phi = 10.9^\circ$  (Seeg, 2017)
- Tiny jet opening angles  $\zeta \Rightarrow$  Seeg, 2017:  $\zeta = 3.4^\circ$
- Single-zone model insufficient
  - Deceleration along jet axis (Georganopoulos and Kazanas, 2003)
  - Spine-Sheath model (Ghisellini et al., 2005)



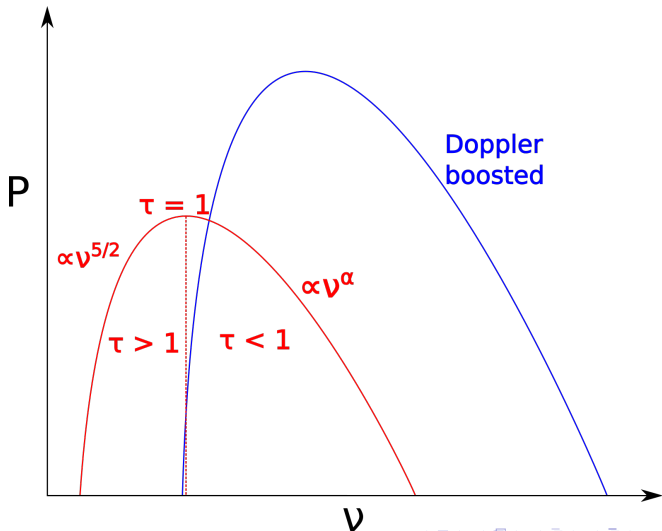
# Summary

- Doppler Crisis: Discrepancy of derived intrinsic Lorentz factors in the  $\gamma$ -rays and the small apparent speeds from kinematic analysis in the radio-frequencies
- Aim is to perform an independent kinematic analysis for TeV blazars from the TANAMI sample
- Extended results to Piner & Edwards gained:
  - Many components stationary or subluminal
  - But: peak velocities at  $\sim 8c$  and  $\sim 6c$
- Further research on Doppler Crisis required
- Inclination of PKS 0625–354 restricted to be between BL Lac and FR 1
- More jet-bending in PKS 2155–304 proposed

# Backup Slides

# Doppler Beaming

Cone-shaped emission of relativistic particles with opening  $\sim \Gamma^{-1}$   
 $D = \nu_{\text{obs}}/\nu_{\text{emit}}$  and  $S(\nu_{\text{obs}}) = D^{3-\alpha} S(\nu_{\text{emit}})$





# Resolution

Smallest resolvable angle is given by Rayleigh criterion

$$\theta \sim \frac{\lambda}{D}, \quad [\theta] = 1 \text{ rad}$$

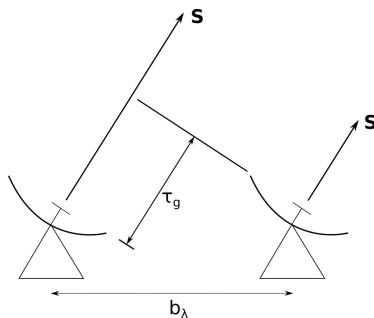
Consider  $\lambda = 3.5 \text{ cm}$  (radio frequencies)  
and  $D = 100 \text{ m}$  (Effelsberg)

$$\Rightarrow \theta \approx 1.2 \text{ arcmin}$$

But we need  $\theta \lesssim 1 \text{ mas}$  for kinematics!  
 $\Rightarrow$  Very Long Baseline Interferometry

# Two-Element Interferometer

Two antennas with geometrical delay  $\tau_g$  and baseline  $b_\lambda$



Interferometer measures the complex visibility:

$$V_{ij} = \int A(\sigma) B_\nu(\sigma) \exp(i2\pi b_{ij,\lambda} \times \sigma) d\Omega$$

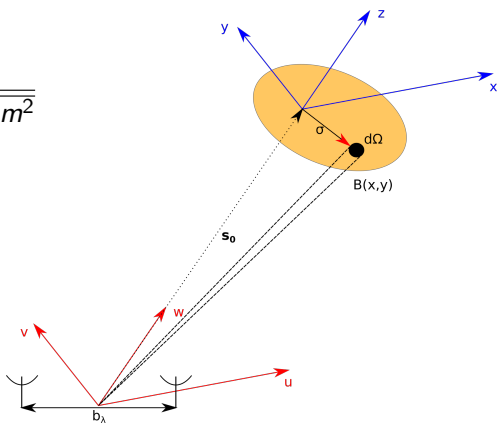
# The $(u, v)$ -plane

$$V_{ij} = \int A(l, m) B_v(l, m) \exp [i2\pi(ul + vm)] \frac{dl dm}{\sqrt{1 - l^2 - m^2}}$$

Small angle approximation:

$$V_{ij} \approx \int A(x, y) B(x, y) \exp [i2\pi(ux + vy)] dx dy$$

$$\Rightarrow B(x, y) \stackrel{\text{FT}}{\rightleftharpoons} V(u, v)$$



# Imaging with CLEAN and SELFCAL

Task: Deconvolution of complex visibility with dirty beam and inverse Fourier transform

Method: Hybrid Imaging

CLEAN algorithm from Högbom, 1974

- Place windows over brightest peaks in dirty image
- Subtraction from dirty image with gain  $\gamma \leq 1$
- repeat until coherent model is found

Reduction of Errors with SELFCAL

$$S = \sum_k \sum_{ij} w_{ij}(t_k) \left| V_{ij}^{\text{cal}} - g_i(t_k) g_j^*(t_k) V_{ij}^{\text{mod}}(t_k) \right|^2$$

Usage of several phase and amplitude selfcals during imaging

# Inclination of PKS 0625–354

Inclination angle given by flux ratio:

$$\phi = \arccos \left[ \frac{1 \left( \frac{S_{\text{jet}}}{S_{\text{counter}}} \right)^{\frac{1}{3-\alpha}} - 1}{\beta \left( \frac{S_{\text{jet}}}{S_{\text{counter}}} \right)^{\frac{1}{3-\alpha}} + 1} \right]$$

Venturi et al., 2000 computes  $\phi < 61^\circ$  and  $\phi < 43^\circ$  with another method

Use flux of inner two components and approximate counter-jet with  $5\sigma$

$\Rightarrow$  average over all epochs

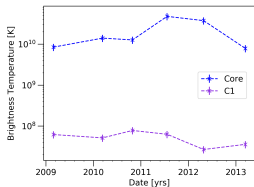
$$\phi < 59^\circ$$

$\Rightarrow$  intermediate object, neither FR 1 nor BL Lac

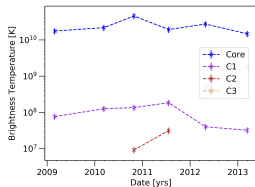
# Brightness Temperatures

$$T_b = \frac{2 \ln 2 S_C \lambda^2 (1+z)}{\pi k_B \theta_{\text{maj}} \theta_{\text{min}}}$$

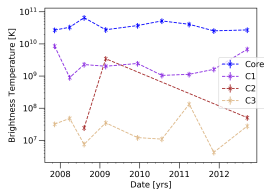
(Kovalev, 2005)



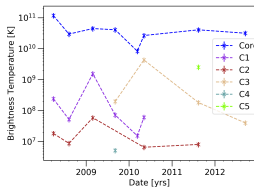
PKS 1440-389



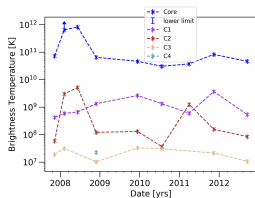
PKS 0447-439



PKS 2005-489



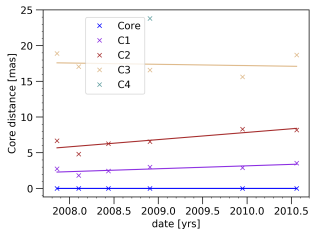
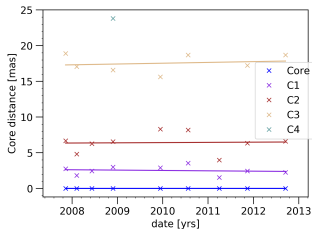
PKS 2155-304



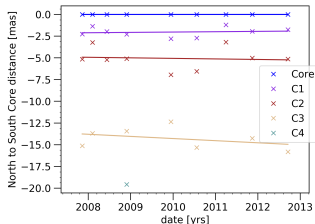
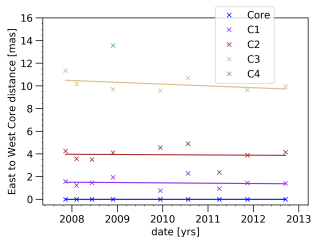
PKS 0625-354

# Fitting with Linear Regression

Radial method and comparison with Trüstedt, 2013:



Separate  $x$ - and  $y$ - fits with subsequent norm computation:



# Apparent Velocities

Two Methods: Radial velocity or vectorial method, i.e. separate  $x$ - and  $y$ -velocities

Source Name	Label	$\beta_{\text{app,rad}}$	$\beta_{\text{app,vec}}$
PKS 1440–389	C1	$-0.03 \pm 0.87$	$0.99 \pm 0.73$
PKS 0447–439	C1	$4.9 \pm 2.2$	$5.4 \pm 2.5$
PKS 2005–489	C1	$0.26 \pm 0.74$	$0.31 \pm 0.41$
	C3	$3.2 \pm 2.6$	$4.3 \pm 2.2$
PKS 2155–304	C1	$5.7 \pm 6.0$	$7.4 \pm 6.0$
	C2	$6.6 \pm 3.1$	$7.8 \pm 2.5$
	C3	$-1.8 \pm 1.4$	$1.7 \pm 1.4$
PKS 0625–354	C1	$-0.18 \pm 0.49$	$0.18 \pm 0.41$
	C2	$0.11 \pm 1.1$	$0.24 \pm 0.96$
	C3	$0.4 \pm 1.1$	$1.07 \pm 0.89$